Borneo International Journal eISSN 2636-9826; Vol. 2 (1); 2019; 16-25
Published by *Majmuah Enterprise*
www.majmuah.com

Using GIMP and ShaderMap Tools as an Alternative Segmentation Method for Retinal Image Enhancement

Sarah Qahtan Mohammed Salih[1], Abdul Sattar Arif Khamas[2]

[1] *Computer Center, College of health and medical technology-Baghdad, Middle Technical University, Iraq*

[2] *Radiology departments, College of health and medical technology-Baghdad, Middle Technical University, Iraq*

Email: sarah.qahtan2014@gmail.com

Received: September 20, 2019
Accepted: October 12, 2019
Online Published: October 12, 2019

Abstract

Retinal image segmentation plays an important role in monitoring and diagnosing retinal diseases. It is considered as one of the most challenging tasks for computer graphics researchers. Many researchers used complex approach to obtain the segmentation of retinal images for medical diagnoses. However, the main goal of this study is proposing an alternative method for segmenting retinal image by employing two tools. ShaderMap and GIMP, the GNU Image Manipulation Program used in this paper for creating normal map that can improve the retinal image and give an alternative of those acquired from segmentation. The performance of the proposed method was evaluated on one high resolution retinal image datasets (REVIEW) and one low resolution image datasets (DRIVE). According to the pre-designed questionnaire, the proposed method improved the retinal image and GIMP gave better result compared to ShaderMap. However, when high resolution retinal image used there was no significant differences between both tools.

Keywords: GIMP, medical visualization, normal mapping, retinal image, segmentation, ShaderMap

1. Introduction

Retinal images refer to the light-sensitive layer of tissue on the back surface of the eye. Assessment of the retinal images considers very important in monitoring and diagnosis visual system diseases such as diabetes (Mendonca & Campilho, 2006; Teng, Lefley, & Claremont, 2002), hypertension (Hammond, Wells, Marcus, & Prisant, 2006) and other diseases. As presented by (Yin, Ng, He, Zhang, & Abbott, 2014) any problem in the blood vessels of the human eye can cause many eye diseases. In computer graphics, computer aided retinal disease screening systems involved the algorithms of "retinal vessel segmentation" to diagnose the retinal disease of visual system. The computer aided systems have been motivated to prevent the manual delineation of retinal blood vessels that needs extensive expertise and training (Yin et al., 2014; You, Peng, Yuan, Cheung, & Lei, 2011).

In computer graphics, the process of separating an image in to several segments (sets of pixels) known as image segmentation. The purpose of this process is to simplify the complexity of an image and make it easy to analyse. Image segmentation is employed to discover the boundaries in an image such as edges, curves, and lines (Lira, 2015). Medical imaging has many segmentation application, in (Yin et al., 2014; You et al., 2011) many approaches are shown about retinal image segmentation and new methods are proposed.

Image segmentation approaches can be quite complicated. In this study we will present some alternative methods, based on the normal mapping, and compare two available tools for image processing, to improve the details of the inner surface of the eye. We will use ShaderMap and GIMP (Team, 2015) to produce normal map images, then we will use each normal map to generate new image by using normal mapping rendering. The final outcome produces an image segmentation effect that can be alternated of those gained from segmentation. Finally, we will compare between the final outcomes from both tools.

2. Related Works

In scientific and medical visualization, normal mapping or bump mapping is used to calculate the texture coordinates of the constructed surface. Then, the texture is applied during visualization. In 2011, a study is proposed such approach that required pre-processing to calculate the surface geometry (Wakid, Kirmizibayrak, & Hahn, 2011). Nonetheless, for the purposes of calculating the surface geometry without any pre-processing isosurface volume rendering is used (Bruder, Frey, & Ertl, 2016; Liu, Clapworthy, & Dong, 2015; Preim & Botha, 2013; Wu, Knoll, Isaac, Carr, & Pascucci, 2017).

Bump mapping is proposed by many researchers in different approaches. Bump mapping and hardware accelerated rendering techniques have recommended by Blinn (Blinn, 1978) to change the normal vector to present a 3D model. Then, the normal vector is employed to calculate light instead of the original normal vector. More complicated approaches take into account the displacement of the sample points and surface height (González, Pérez, & Orduña, 2017; Khoshkhou et al., 2016; Luetkemeyer, Cai, Neu, & Arruda, 2018).

Normal mapping is mostly used in bump map approaches, where normal vectors are pointed in the positive z direction in tangent space. The z direction is the normal vector N in the tangent space, the x and y direction in the world space converted to T and B vectors in the tangent space as shown in Figure 1. The T is the (1, 0) vector which is correspond to (u) in texture space and The B is the (0, 1) vector which is correspond to (v) in texture space. The matrix below is built from the T, B, N vectors and for the light (n) calculation in the world space. The range of the texture normal vector (norm) must normalize between -1 and 1 .The following equation (1) is transferred the tangent space to the world space by multiplying the texture normal vector (norm), by the TBN matrix, where n is used for illumination calculation:

$$n = \begin{bmatrix} Tx & Ty & Tz \\ Bx & By & Bz \\ Nx & Ny & Nz \end{bmatrix} * \begin{bmatrix} norm\ x \\ norm\ y \\ norm\ z \end{bmatrix} \quad (1)$$

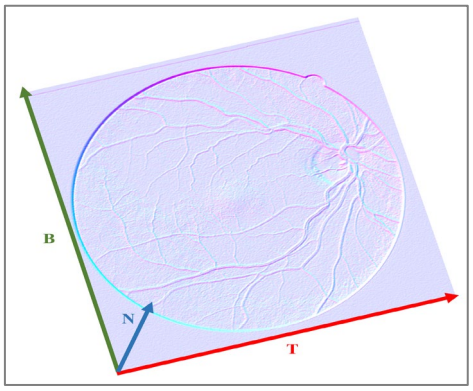

Figure 1: shows the tangent space for the retinal image

The first step in normal mapping rendering is generating the normal map, for this aim researchers employed many tools such as GIMP (Conegliano & Schulze, 2016; Innamorati, Ritschel, Weyrich, & Mitra, 2017; Lai, Yeung, Yan, Fu, & Tang, 2016; Sparavigna, 2015; Verhoeven, 2017; Zeng et al., 2019), Blender, Unity, ShaderMap and several other application.

Sparavigna in 2014 and 2015 used Sobel filter and other filters in GIMP to enhance medical images (Sparavigna, 2014, 2015). In 2008, Sulaiman used ITK-SNAP tool to enhance liver images and to remove noise that can emphasize the liver region by changing the contrast (Sulaiman, Rahmat, Mahmod, & Rashid, 2008). In 2014, Candiago and Kawamoto used ShaderMap program to create normal maps from textures (Candiago & Kawamoto Júnior, 2014). Agyemang employed the program to fake the depth and create realistic scenes by generating the specular, ambient occlusion and normal maps (Agyemang, 2016). In this paper, we propose normal mapping rendering for enhancing retinal image by employing two tools for generating normal map textures which are GIMP and ShaderMap.

2.1 GIMP and ShaderMap

GIMP is open source and free of charge image processing and drawing tool. It can be used as most image editor for converting image formats, adjust brightness and contrast, cropping and resizing images. GIMP supports many plug-ins that can increase its capability for editing images. Basically, GIMP can edit an image by creating layers of it in a stack just like Photoshop. The toolbox has suitable filters for edge detections such as Sobel and Laplace. Furthermore, GIMP can provide many filters and effects that can be sharp and blur images. GIMP can import and export most common formats such as GIF, JPEG, BMP, PNG and TIFF.

ShaderMap is texture creation tool that can convert 2D images or 3D models to the prevalent texture maps, like normal, displacement map, ambient occlusion and specular . It provides displacement and albedo maps from diffuse, normal map from displacement map, displacement map and ambient occlusion from 3d model. Some maps do not have an input while others have more than one input. In addition, this tool provides a map that can combine all the other maps. ShaderMap native formats are designed to store all detail information about an image. It supports image formats such as GIF, PNG, BMP, JPEG and TIFF and other format such as PSD and TGA. Also, it exports files like PNG, PSD, TGA, BMP and JPG by taking screenshot to the last modification in the program.

3. Methodology

The method presented in this paper is based on the normal mapping by generating normal map using two tools (GIMP and ShaderMap) that can be used as an alternative method to the retinal images segmentation. Figure 2 shows a framework for the normal mapping process; following the details of our method will discuss in steps as demonstrated in this Figure 2.

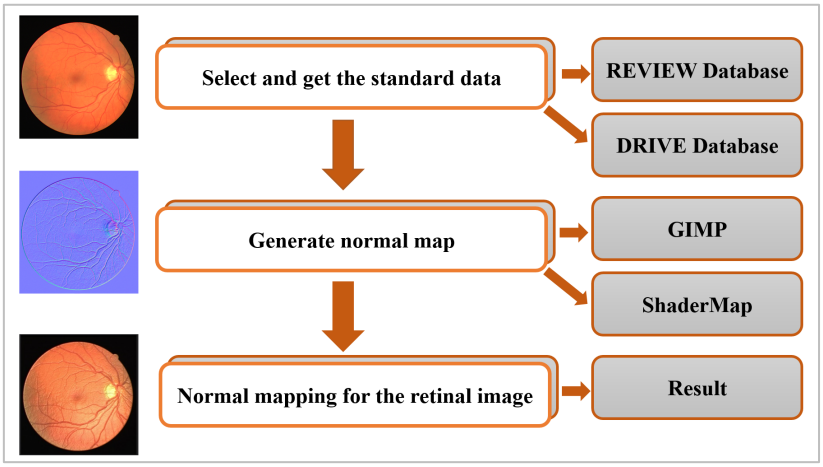

Figure 2: the framework of the proposed method

3.1 Retinal Images Databases

Researchers used standard datasets to validate medical image processing algorithms by comparing their result to result obtained by the experts. In this paper, we use digital images from two free databases available online which are REVIEW (Al-Diri, Hunter, & Steel, 2009) and DRIVE (Staal, Abràmoff, Niemeijer, Viergever, & Van Ginneken, 2004).

The REVIEW database has 16 images categorized into 4 sets which are CLRIS, HRIS, KPIS and VDIS. The sets have 2,4,2 and 8 images, respectively, the resolution ranges are from 1360×1024 to 3584×2438 pixels. Canon EOS D30 used to acquire this dataset with focal length 50mm.

The DRIVE database has 40 colour retinal images categorized into 20 images in test set and 20 images in training set. All the image dimensions were cropped to 565×584 pixels, the resolution set to 96 dpi, compressed in LZW as TIFF format. Canon CR5 non-mydriatic three CCD camera was used to acquire the images and the field of view (FOV) set to 45 degree.

3.2 Normal Map Texture Generation

Our method is started by generating normal map texture using GIMP and ShaderMap. The procedure of creating the textures by the two tools is explained in Section 3.2.1.

3.2.1 GIMP Procedure

1. Open the colour retinal images.
2. Duplicate the current layer and Desaturate the selected image from colour tab then select Luminance mode.
3. Duplicate the desaturated image then manipulate the intensity of the grey level by using Curves in the colour tab.
4. Convert the last modified image to normal map from Filter tab and Map command. The normal map filter gave an option to increase or decrease the details of the texture as shown in Figure 3 by changing the scale option.
5. The last step was exporting the normal map image and the desaturated image as JPEG format.

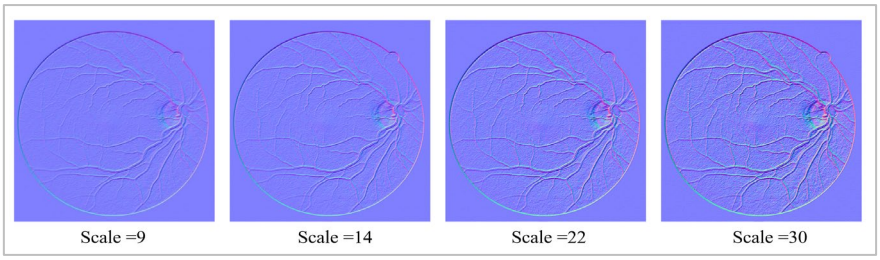

Figure 3: Illustrated the scale level of normal map filter in GIMP

3.2.2 ShaderMap Procedure

1. Select the standard mode of the texture and the colour texture or the displacement map at the interface of the application.
2. Select the image that we want to generate normal map texture for it.
3. Select the normal map from the project grid to enable the modification of the texture.
4. Manipulate the normal map setting to get the satisfied result by changing the intensity command depending on the input image used and the available details.
5. Save the normal map and the displacement textures for the next step in JPEG format.

The normal map could be generated by using colour texture or the displacement map. We noticed the result of the colour texture had less details and looked blur as shown in Figure 4. All the options kept as default to show the different between the two selected options for generating normal map.

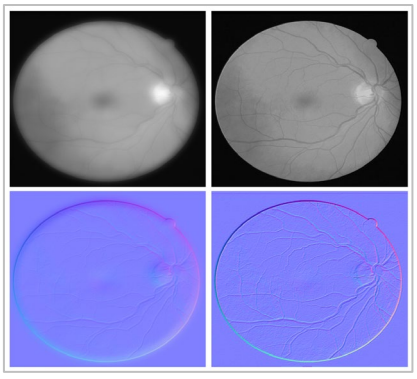

Figure 4: Difference between using the left: colour texture and the right: displacement map

3.3 Normal Mapping of Retinal Image

Our proposed rendering method, take two images as an input the colour (diffuse) image and the normal map image as shown in Figure 5. The tangent space used to calculate normals in normal maps, then they were transformed to world space to calculate lights.

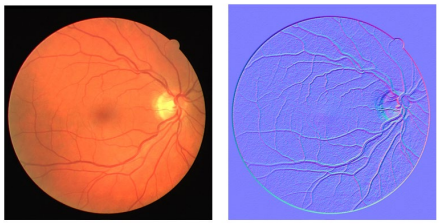

Figure 5: Input images in the normal mapping rendering phase

Suppose there are 3 points P1, P2 and P3 on a surface, that as represented P1(u1, v1), P2(u2, v2) and P3(u3, v3), respectively. The direction of T (tangent vector) and B (bitangent vector) that shown in Figure 1 line up with the direction of surface's texture coordinates that shown in Figure 6. Where edge E1 that define as ΔU1and ΔV1 are aligned with T and B vectors. From this fact the edges E1and E2 can be found and the detail procedure for finding tangents and bitangents shown in Figure 6:

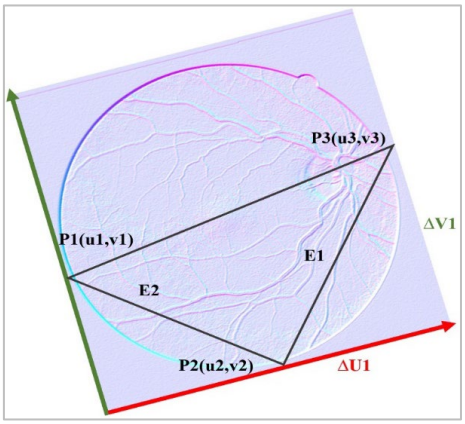

Figure 6: Illustration of texture coordinates in tangent space

1. The texture coordinates uv1, uv2, uv3 and uv4 were assumed to be (0.0, 1.0), (0.0, 0.0), (1.0, 0.0) and (1.0, 1.0).
2. The normal vector was assumed to be (0.0, 0.0,1.0).
3. The edges in tangent and bitangent were calculated by equation (2)

$$\begin{aligned} E1&=P3-P2 \\ E2&=P1-P2 \end{aligned} \qquad (2)$$

4. The textures in tangent and bitangent were calculated by equation (3)

$$\begin{aligned} \Delta UV1 &= uv3 - uv2 \\ \Delta UV2 &= uv1 - uv2 \end{aligned} \qquad (3)$$

5. The tangent for the two triangles calculated by equation (4)

$$\begin{aligned} Tx &= 1.0 / (\Delta UV1.x * \Delta UV2.y - \Delta UV2.x * \Delta UV1.y) * (\Delta UV2.y * E1.x - \Delta UV1.y * E2.x) \\ Ty &= 1.0 / (\Delta UV1.x * \Delta UV2.y - \Delta UV2.x * \Delta UV1.y) * (\Delta UV2.y * E1.y - \Delta UV1.y * E2.y) \\ Tz &= 1.0 / (\Delta UV1.x * \Delta UV2.y - \Delta UV2.x * \Delta UV1.y) * (\Delta UV2.y * E1.z - \Delta UV1.y * E2.z) \end{aligned} \qquad (4)$$

6. The bitangent for the two triangles calculated by equation (5)

$$\begin{aligned} Bx &= 1.0 / (\Delta UV1.x * \Delta UV2.y - \Delta UV2.x * \Delta UV1.y) * (-\Delta UV2.x * E1.x + \Delta UV1.x * E2.x) \\ By &= 1.0 / (\Delta UV1.x * \Delta UV2.y - \Delta UV2.x * \Delta UV1.y) * (-\Delta UV2.x * E1.y + \Delta UV1.x * E2.y) \\ Bz &= 1.0 / (\Delta UV1.x * \Delta UV2.y - \Delta UV2.x * \Delta UV1.y) * (-\Delta UV2.x * E1.z + \Delta UV1.x * E2.z) \end{aligned} \qquad (5)$$

All the previous calculations were passed to the vertex shader to create TBN matrix. The input to the vertex shader were points positions, normal, texture coordinate, tangent and bi tangent and the output were fragment (surface) position, texture coordinate, the position of light, view and fragment in the tangent space.

1. The TBN matrix created by the calculations represented by equation (6):

$$\begin{aligned} N &= \text{Normal Matrix} \times \text{Normal vector} \\ T &= \text{Normal Matrix} \times \text{Tangent} - (\text{Normal Matrix} \times \text{Tangent}.N) \times N \\ B &= N \times T \\ TBN &= \text{transpose the matrix } (T, B, N) \end{aligned} \quad (6)$$

   The last steps in vertex shader were calculating light, view and fragment in the tangent space by multiply them with TBN matrix.
2. In the fragment shader, the normal obtained from normal map in range [0,1] and then transform to range [-1,1] which represent the normal in tangent space.
3. Two lights were set up (above and under) the textures to show the impact of the normal mapping.
4. Finally, all the colours and lighting calculations were done based on Blinn (Blinn, 1978).

The final result can be shown in Figure 7 where (a) is the original image (b) and (c) are the normal map using ShaderMap and GIMP, (d) and (e) is final result of our proposed method.

4. Result and Discussion

All the experiments are carried out on a laptop Lenovo Y50 running Windows 10 with an Intel(R) Core(TM) i7- 4710HQ CPU (2.50 GHz) and 16 GB of memory. The algorithm has been implemented in visual C++ programming language, OpenGL 4.0 library. The normal maps were created using GIMP 2.10.8 and ShaderMap R2 version 4.2.3.

Normally, the segmentation methods compared with ground truth that can be generated by one or more experts in the field of study. Also, some researchers used a pre-designed questionnaire to test the validity of their proposed method. In this section, we are reported qualitative results. The aim of the qualitative comparison was providing a visual appreciation for the superiority of the normal mapping rendering by using GIMP and ShaderMap of the retinal image.

Four high resolution images were selected for our experiment from REVIEW (HRIS category) and four images from DRIVE (training set). The questionnaires were given to bachelor students of the optics techniques in the College of Health and Medical Technology, Middle Technical University, to be completed. The questionnaires was carried out by 156 students from different stages in age 22-24 and constituted 68 male and 88 female. The questionnaire was written in English and a brief presentation was given to the student to help them understand each question. The questionnaire categorized to three sections which are preference rate, 3D effect and the fidelity. Likert scale was selected to rate their response and the scores are classified as 5 levels as used by many researchers (Harpe, 2015; Joshi, Kale, Chandel, & Pal, 2015; Series, 2012). Level 5 indicates "strongly agree" to level 1 that represents “strongly disagree”.

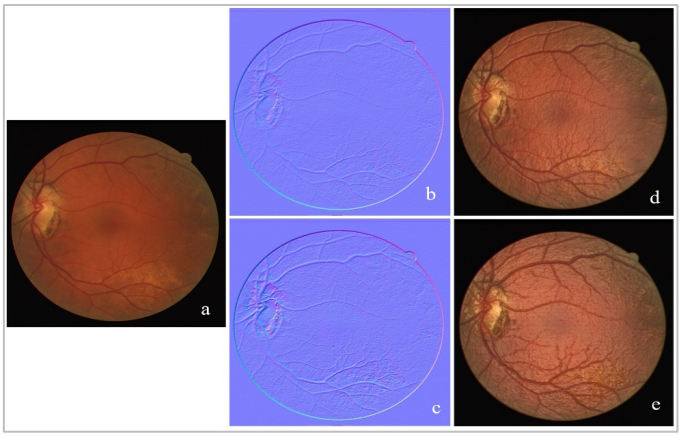

Figure 7: Normal mapping of retinal image and segmentation results: (a) original images, (b) normal map using ShaderMap, (c) normal map using GIMP, (d) and (e) final result of our proposed method.

The first category of the questionnaire started by asking the respondents about their preference of the retinal images that generated by the proposed method as shown in Figure 7, no matter how the reality it is. The evaluations of the preference rate are plotted as Figure 8, from which we find the highest score was awarded to the GIMP with 44 against ShaderMap with 37 scores. Agree scores were given to GIMP and ShaderMap with 34 and 32 scores respectively. However, 30 scores were neither agree nor disagree about GIMP against 28 to ShaderMap. In contrast, ShaderMap got 23 and 36 scores were strongly disagree and disagree respectively. Alike, GIMP got 22 and 26 scores. The overall preference rate was 50 percent for GIMP against the ShaderMap which was 44 percent. However, disagree rate was 31 percent for GIMP against 38 percent for the ShaderMap.

The second category of the questionnaire was the 3D effect, where the respondents were asked to score their opinion about the 3D effect of the retinal image created by GIMP and ShaderMap. The scores selected by the respondents for GIMP were 50, 70, 18, 15 and 3 for strongly agree, agree, neutral, disagree and strongly disagree respectively. Nevertheless, ShaderMap got 41, 55, 30, 20 and 10 scores. The highest score rate was four, demonstrating that most of the respondents believed the GIMP gave high 3D effect and overall responses rate was 77 percent against 62 percent for ShaderMap. On the other hand, the overall disagree rate was 12 percent against 19 percent for ShaderMap. The students believed that both tools gave the feeling of depth to the image.

The last category in the questionnaire was the fidelity, the scores represent the result of comparing the images generated from GIMP and ShaderMap with the original images. The score of the comparing GIMP with the original image was strongly agree with 54 score and ShaderMap with 44 score. Agree was selected by 60 respondents for GIMP and 50 respondents for ShaderMap. The neutral respondents were 20 and 30 for GIMP and ShaderMap respectively. Finally, Gimp got 18 and 4 for disagree and strongly disagree respectively. In the same order ShaderMap got 22 and 10. The respondents gave 73 percent of their result to GIMP compared to the original image. However, 60 percent of the result went with ShaderMap. The overall disagree rates were 14 and 21 percent for GIMP and ShaderMap respectively. The participants believed in the accuracy of GIMP to create the normal map to enhance the retinal image.

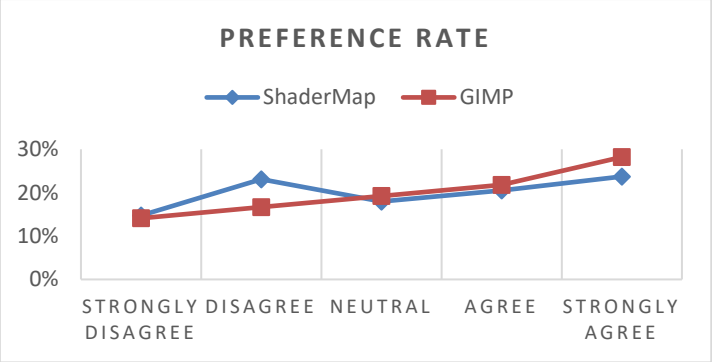

Figure 8: The preference rate of GIMP and ShadeMap

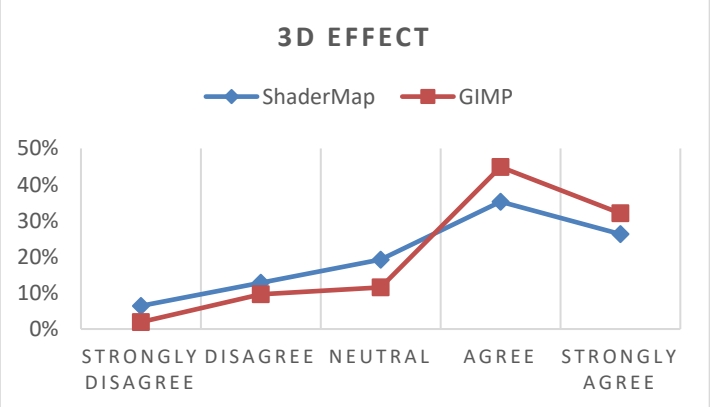

Figure 9: The 3D effect of GIMP and ShadeMap

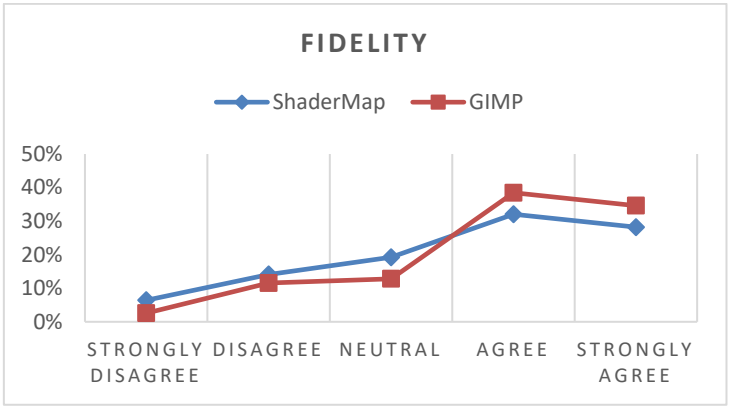

Figure 10: Fidelity GIMP and ShadeMap compared to the original image

The method proposed in this study has proved to be a valuable as an alternative segmentation tool. Similar to the study presented by Sparavigna (Sparavigna, 2014), where she used GIMP, Iris and AstroFracTool to segment the retinal image. However, Sparavigna used GIMP to create bump mapping for the fundus of the eye. From the experiment, we noted that there was no significant differences between GIMP and ShaderMap on data REVIEW as shown in Figure 11. Conversely, GIMP reported to be better segmentation tool when we used DRIVE dataset see Figure 12. The only difference between the two dataset are the resolution of the images. In addition, the REVIEW data took more executing time than DRIVE data.

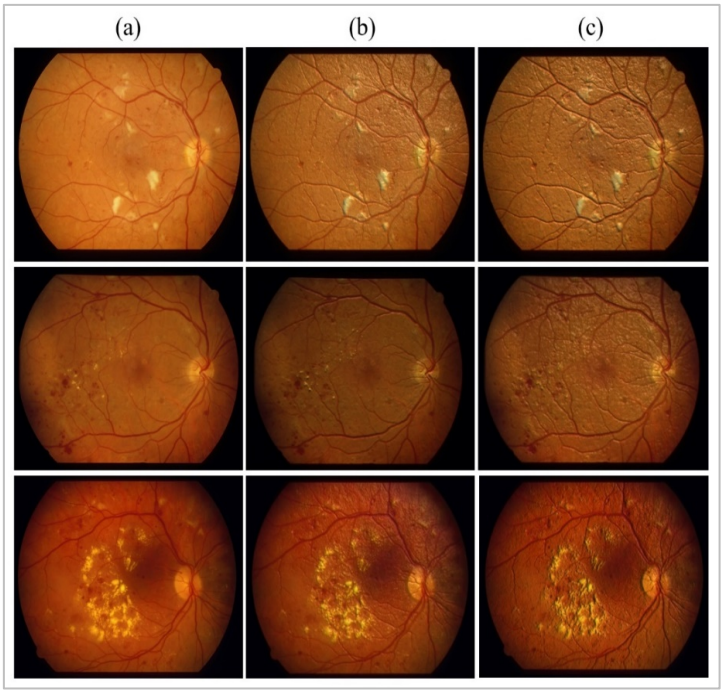

Figure 11: The result of proposed method on sample from REVIEW dataset, (a) original image; (b) obtained by using ShaderMap; (c) obtained by using GIMP

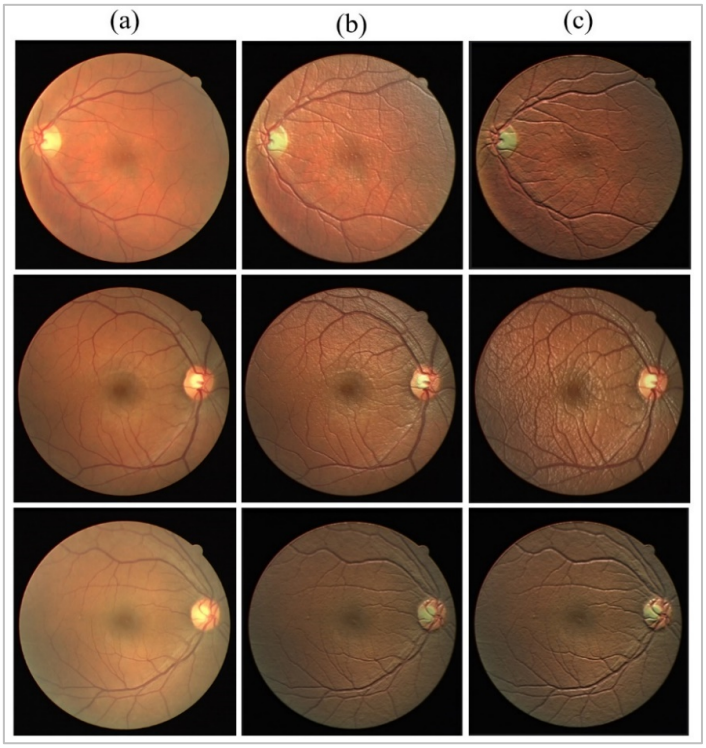

Figure 12: The result of proposed method on sample from DRIVE dataset, (a) original image; (b) obtained by using ShaderMap; (c) obtained by using GIMP

5. Conclusion

The two tools employed in this paper are able to enhance the retinal images. In addition, it is able to give an alternative segmentation method of the retinal images. Our segmentation approach could help in diagnosis and monitoring retinal diseases. Both tools are based on grey tone images and ShaderMap seems easy, simple to use and diffuse image can be used to create normal map. Nevertheless, GIMP seems able to give more details of retinal images as shown in Figure 12. The normal map that created by both tool can be improved by manipulating and adjusting the grey level of the diffuse image.

Acknowledgments

The authors would like to thank the authors of DRIVE and RIVIEW databases for making their data publicly available.

References

Agyemang, S. A. (2016). Improving the interactivity of chemistry in junior and senior secondary schools in Ghana through virtual reality.

Al-Diri, B., Hunter, A., & Steel, D. (2009). An active contour model for segmenting and measuring retinal vessels. IEEE transactions on medical imaging, 28(9), 1488-1497.

Blinn, J. F. (1978). Simulation of wrinkled surfaces. Paper presented at the ACM SIGGRAPH computer graphics.

Bruder, V., Frey, S., & Ertl, T. (2016). Real-time performance prediction and tuning for interactive volume raycasting. Paper presented at the SIGGRAPH ASIA 2016 Symposium on Visualization.

Candiago, A., & Kawamoto Júnior, L. T. (2014). Virtual Multimedia Environment to Teach Safety Procedures in Laboratories. Paper presented at the Advanced Materials Research.

Conegliano, A., & Schulze, J. P. (2016). Realistic 3D Modeling of the Liver from MRI Images. Paper presented at the International Symposium on Visual Computing.

González, C., Pérez, M., & Orduña, J. M. (2017). Combining displacement mapping methods on the GPU for real-time terrain visualization. The Journal of Supercomputing, 73(1), 402-413.

Hammond, S., Wells, J. R., Marcus, D. M., & Prisant, L. M. (2006). Ophthalmoscopic findings in malignant hypertension. The Journal of Clinical Hypertension, 8(3), 221-223.

Harpe, S. E. (2015). How to analyze Likert and other rating scale data. Currents in Pharmacy Teaching and Learning, 7(6), 836-850.

Innamorati, C., Ritschel, T., Weyrich, T., & Mitra, N. J. (2017). Decomposing single images for layered photo retouching. Paper presented at the Computer Graphics Forum.

Joshi, A., Kale, S., Chandel, S., & Pal, D. (2015). Likert scale: Explored and explained. British Journal of Applied Science & Technology, 7(4), 396.

Khoshkhou, D., Mostafavi, M., Reinhard, C., Taylor, M., Rickerby, D., Edmonds, I., . . . Connolly, B. (2016). Three-dimensional displacement mapping of diffused Pt thermal barrier coatings via synchrotron X-ray computed tomography and digital volume correlation. Scripta Materialia, 115, 100-103.

Lai, C.-F. W., Yeung, S.-K., Yan, X., Fu, C.-W., & Tang, C.-K. (2016). 3D navigation on impossible figures via dynamically reconfigurable maze. IEEE transactions on visualization and computer graphics, 22(10), 2275-2288.

Liu, B., Clapworthy, G. J., & Dong, F. (2015). IsoBAS: a binary accelerating structure for fast isosurface rendering on GPUs. Computers & Graphics, 48, 60-70.

Luetkemeyer, C. M., Cai, L., Neu, C. P., & Arruda, E. M. (2018). Full-volume displacement mapping of anterior cruciate ligament bundles with dualmri. Extreme Mechanics Letters, 19, 7-14.

Mendonca, A. M., & Campilho, A. (2006). Segmentation of retinal blood vessels by combining the detection of centerlines and morphological reconstruction. IEEE transactions on medical imaging, 25(9), 1200-1213.

Preim, B., & Botha, C. P. (2013). Visual computing for medicine: theory, algorithms, and applications: Newnes.

Series, B. (2012). Methodology for the subjective assessment of the quality of television pictures. Recommendation ITU-R BT, 500-513.

Sparavigna, A. C. (2014). GIMP and wavelets for medical image processing: Enhancing images of the fundus of the eye. arXiv preprint arXiv:1408.4703.

Sparavigna, A. C. (2015). An image processing approach based on Gnu Image Manipulation Program Gimp to the panoramic radiography. International Journal of Sciences, 4(5), 57-67.

Staal, J., Abràmoff, M. D., Niemeijer, M., Viergever, M. A., & Van Ginneken, B. (2004). Ridge-based vessel segmentation in color images of the retina. IEEE transactions on medical imaging, 23(4), 501-509.

Sulaiman, P. S., Rahmat, R. W., Mahmod, R., & Rashid, A. (2008). A liver level set (LLS) algorithm for extracting liver's volume containing disconnected regions automatically. IJCSNS, 8(12), 246.

Team, G. (2015). GIMP-The GNU Image Manipulation Program. Online. URL https://www. gimp. org.

Teng, T., Lefley, M., & Claremont, D. (2002). Use of two-dimensional matched filters for estimating a length of blood vessels newly created in angiogenesis process. Medical & Biological Engineering & Computing, 40, 2-13.

Verhoeven, G. J. (2017). COMPUTER GRAPHICS MEETS IMAGE FUSION: THE POWER OF TEXTURE BAKING TO SIMULTANEOUSLY VISUALISE 3D SURFACE FEATURES AND COLOUR. ISPRS Annals of Photogrammetry, Remote Sensing & Spatial Information Sciences, 4.

Wakid, M., Kirmizibayrak, C., & Hahn, J. K. (2011). Texture mapping volumes using GPU-based polygon-assisted raycasting. Paper presented at the 2011 16th International Conference on Computer Games (CGAMES).

Wikipedia. (2019). Image Segmentation Retrieved from https://en.wikipedia.org/wiki/Image_segmentation

Wu, K., Knoll, A., Isaac, B. J., Carr, H., & Pascucci, V. (2017). Direct Multifield Volume Ray Casting of Fiber Surfaces. IEEE transactions on visualization and computer graphics, 23(1), 941-949.

Yin, X., Ng, B. W., He, J., Zhang, Y., & Abbott, D. (2014). Accurate image analysis of the retina using hessian matrix and binarisation of thresholded entropy with application of texture mapping. PLoS One, 9(4), e95943.

You, X., Peng, Q., Yuan, Y., Cheung, Y.-m., & Lei, J. (2011). Segmentation of retinal blood vessels using the radial projection and semi-supervised approach. Pattern Recognition, 44(10-11), 2314-2324.

Zeng, Y., Rao, B., Chapman, W. C., Nandy, S., Rais, R., González, I., . . . Zhu, Q. (2019). The Angular Spectrum of the Scattering Coefficient Map Reveals Subsurface Colorectal Cancer. Scientific reports, 9(1), 2998.